From 1965–1966, he was employed at the Bell Telephone Laboratories, Holmdel, NJ, while on leave from the University of Utah. During this time, he worked in the area of microwave avalanche diode oscillators.

Again, in 1971, he was engaged in study and research involving microwave biological effects at the University of Washington Seattle, while on leave from the University of Utah. From 1977 to 1982, he was chairman of the Electrical Engineering Department at the University of Utah, where he is presently Professor of Electrical Engineering and engaged in teaching and research in electromagnetics, engineering pedagogy, and microwave biological effects.

Dr. Durney is a member of The Bioelectromagnetics Society, Commission B of URSI (International Union of Radio Science), Sigma Tau, Phi Kappa Phi, Sigma Pi Sigma, Eta Kappa Nu, and the American Society for Engineering Education. He also served as Vice President (1980–1981) and President (1981–1982) of The Bioelectromagnetics Society, as a member (1979–present) and Chairman (1983–present) of the IEEE Committee on Man and Radiation (COMAR), as a member of the American National Standards Institute C95 Subcommittee IV on Radiation Levels and/or Tolerances with Respect to Personnel (1973–present), as a member of the editorial board of the IEEE TRANSACTIONS ON MICROWAVE THEORY AND TECHNIQUES (1977–present), and as a member of the editorial board of *Magnetic Resonance Imaging* (1982–present). In 1980, he received the Distinguished Research Award from the University of Utah, and the Outstanding Teaching Award, College of Engineering, University of Utah. In 1982, he received the American Society for Engineering Education Western Electric Fund Award. He was named a College of Engineering Distinguished Alumnus by Utah State University in 1983.

✤

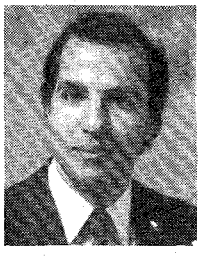

Magdy F. Iskander (S'72–M'76) was born in Alexandria, Egypt, on August 6, 1946. He received the B.Sc. degree in electrical engineering, University of Alexandria, Egypt, in 1969. He entered the Faculty of Graduate Studies at the University of Manitoba, Winnipeg, Manitoba, Canada, in September 1971, and received the M.Sc. and Ph.D. degrees in 1972 and 1976, respectively, both in microwaves.

In 1976, he was awarded a National Research Council of Canada Postdoctoral Fellowship at the University of Manitoba. Since March 1977, he has been with the Department of Electrical Engineering and the Department of Bioengineering at the University of Utah, Salt Lake City, where he is currently an Associate Professor of Electrical Engineering. In 1981, he received the University of Utah President David P. Gardner Faculty Fellow award and spent the academic quarter on leave as a Visiting Associate Professor at the Department of Electrical Engineering and Computer Science, Polytechnic Institute of New York, Brooklyn, N Y.

Dr. Iskander edited two special issues of the *Journal of Microwave Power*, one on "Electromagnetics and energy applications," March 1983, and the other on "Electromagnetic techniques in medical diagnosis and imaging," September 1983. He has contributed chapters to four research books and has published in technical journals and presented more than 130 papers. In 1983, he received the College of Engineering Outstanding Teaching Award and the College Patent Award for creative, innovative, and practical invention. In 1984, he was selected by the Utah Section of IEEE as the Engineer of the Year. He is a member of the editorial board of the IEEE TRANSACTIONS ON MICROWAVE THEORY AND TECHNIQUES and a member of the editorial board of the *Journal of Microwave Power*. His present fields of interest include the use of numerical techniques in electromagnetics to calculate scattering by dielectric objects, antenna design, and the evaluation of the biological effects as well as the development of medical applications of electromagnetic energy.

Average SAR and SAR Distributions in Man Exposed to 450-MHz Radiofrequency Radiation

ARTHUR W. GUY, FELLOW, IEEE, CHUNG-KWANG CHOU, MEMBER, IEEE, AND BARRY NEUHAUS

Abstract—**Fifth-scale phantom models were exposed to 2450-MHz electromagnetic fields to obtain the average specific absorption rate (SAR) and SAR distribution in man exposed to 1 mW/cm^2 450-MHz radiofrequency radiation for various polarizations and body positions. The average SAR was measured calorimetrically and SAR distribution was determined thermographically using an interactive computer system. The mean SAR, as averaged over the body, remained relatively constant at 0.050 W/kg, with a standard deviation of ±0.007 W/kg for all polarizations and body postures considered in the study. Peak SAR values were as high as 0.650 W/kg, occuring typically in the wrist.**

Manuscript received October 12, 1983; revised March 4, 1984. This research was supported by the Air Force School of Aerospace Medicine (USAF/SAM), Brooks Air Force Base, TX 78235 under Contract F33615-80-C-0612.

The authors are with Bioelectromagnetics Research Laboratory. RJ-30, University of Washington, Seattle, WA 98195.

I. INTRODUCTION

AS ONE PART of a project for evaluating the health of laboratory rats exposed under conditions simulating those of human exposure in order to assess the effects of long-term low-level 450-MHz radiofrequency radiation (RFR) on man [7], this paper reports the measurement of the average specific absorption rate (SAR) of energy and the SAR distribution in man under various conditions of exposure.

Basically, the same techniques were used in these studies as had been previously reported [6]. Approximately 1/4- to 1/10-scaled models of man composed of synthetic muscle tissue were exposed to frequencies from 4 to 10 times higher than the exposure frequency for a full-sized man. In

0018-9480/84/0800-0752$01.00 ©1984 IEEE

TABLE I
CHARACTERISTICS OF SCALE MODELS (SYNTHETIC TISSUES) FOR SIMULATING 450-MHz EXPOSURE AT 2450-MHz RFR

Full-Scale Dielectric Constant ($T=37^{\circ}C$)	Scale Synthetic Tissue	Composition % Total Weight						Scale Dielectric Constant ($T=20^{\circ}C$)	Specific Heat (kcal/kg $^{\circ}C$)	Density (g/cm^3)
		H_2O	Ethylene Glycol	NH_4Cl	NaCl	PEP	TX150			
$\varepsilon'=53$ $\sigma = 1.18$	Muscle (gel)	82			4.2	5.8	8.0	$\varepsilon'=53.3$ $\sigma = 6.4$	.86	1.000
$\varepsilon'=53$ $\sigma = 1.18$	Muscle (liquid)	53.9	40.6	5.5				$\varepsilon'=50.2$ $\sigma = 6.4$	.87	1.074
$\varepsilon'=33$ $\sigma =0.88$	Mixture (liquid: 2/3 muscle; 1/3 fat)	29	65.2	5.8				$\varepsilon'=33.1$ $\sigma = 4.8$	.71	1.099

*Scale Factor—5.44

the scaled models, SAR was measured by a calorimetric system and SAR distribution by a thermographic system; then the values for a full-sized man were obtained by extrapolation. The entire system was modernized to enable the use of digital data-collecting techniques. Software was also developed for greater efficiency and accuracy in processing and printing of the thermogram images.

The study consisted of the following three major tasks:

1) Determination by calorimetry of the values for the average SAR in man for different body postures and sizes under conditions simulating free-space exposure to 450 MHz.

2) Development of an interactive computer system for analysis and processing of thermograph images of exposed phantom scale-models of man to reflect actual SAR distribution patterns (previous thermographs displayed temperature patterns only) and formulation of a computer program for rapid retrieval of SAR values from a large data base.

3) Determination of SAR distributions in man for different body postures and sizes under exposure conditions simulating free-space exposure to 450-MHz.

II. EXPERIMENTAL METHODOLOGY

A.) Exposure Facilities

For relating biological effects observed in rats exposed to RFR in the waveguide system to possible unsafe exposure levels for man, the dosimetry information for the rats exposed in the waveguides had to be correlated to that obtained for humans exposed to free-field 450-MHz 1-mW/cm^2 radiation. Using the facilities of the large anechoic camber [6], dosimetry information was obtained for full-scale man from approximately 1/5-scale models of man fabricated from synthetic tissue (with the same dielectric properties as human tissue), with proper modifications for the scaling factor. Using a scaling factor (SF) of 5.44 (inverse of the reduction factor from the full-scale man to the scale-model man), the models were exposed to 2450-MHz radiation in the anechoic chamber for simulation of a full-scale man exposed to 450-MHz RFR. Previous work of this type had been conducted in the chamber, but exposure levels had been limited to 350 mW/cm^2 because the maximum output of the power source was 2.5 kW. The thermographic technique required relatively short exposure times to maintain maximum accuracy of results (to reduce the effect from diffusion of thermal energy from hot to cooler areas). Therefore, at the outset, it was decided to reduce exposure times by increasing the output of the power source by a factor of four by replacing the existing 2450-MHz 2.5-kW magnetron with an 1800–2450-MHz 10-kW klystron. Incident power density in the anechoic chamber was measured with the NBS (model EDM-1C) energy density meter and the Narda (model 8635) power density meter. The NBS meter measurement was in agreement with theoretical values, but the Narda meter measurement was 13 percent less. Since the guaranteed calibration accuracy of the meters was no better than ± 1 dB, according to the Bureau of Radiological Health, it was decided that using the theoretical gain of the horn (corrected for near-zone field) of 13.9 dB and a carefully calibrated coaxial directional coupler would provide a more reliable prediction of the power density than the meters. All data reported in the following sections are based on the theoretical input power as measured by the calibrated Microlab/FXR CB-68LN coaxial directional coupler attached to a coax-to-waveguide adaptor connected to the standard gain horn.

B.) Synthetic Tissues for Scale Models

To simulate the exposure of a full-scale man to 450 MHz, a suitable synthetic tissue with proper dielectric constant to match the scaling criteria was needed. The scaling conditions [12] pertinent to developing phantom muscle mixtures are

$$\epsilon' = \epsilon \tag{1}$$

and

$$\tan\delta' = \tan\delta \tag{2}$$

where ϵ is the relative permittivity, $\tan\delta$ is the loss tangent, the prime quantities refer to the scale-model system, and the unprimed quantities specify the full-scale system. Since

$$\tan\delta = \sigma/2\pi f\epsilon\epsilon_0 \quad (3)$$

where σ is the conductivity (S/m) and f is the frequency (Hz), the scaling condition for conductivity was derived as

$$\sigma' = \mathrm{SF} \times \sigma. \quad (4)$$

The dielectric properties of the full-scale and scaled models are shown in Table I. The only difference between them is that the electrical conductivity of the latter is increased by the SF. The dielectric properties for the scale-model tissues were measured under controlled-temperature conditions of 20°C. The properties were obtained by transmission-line methods described by [5], [6]. In addition to the scaled liquid muscle, a scaled liquid tissue was used, with the properties of a homogeneous mixture of muscle, fat, and bone representative of the human body with an electrical conductivity of two-thirds that of muscle as described in [2].

C.) *Average SAR's in Spherical Models*

To test the validity of the dielectric property measurements and the calibration of the anechoic chamber, the SAR in a number of spherical models with radii measuring between 2 and 6 cm was determined. The average SAR in watts/kilogram was calculated from the increase in temperature, in the manner described by [6], by the following equation:

$$\mathrm{SAR}_{\mathrm{avg}} = 4.184 \times 10^3\, c\Delta T/\Delta t \quad (5)$$

where c is the specific heat in kcal/kg·°C, ΔT is the temperature increase due to exposure in degrees C, and Δt is the exposure time in seconds. The calculated values are in agreement with the theoretical values obtained by evaluation of the Mie-theory equations developed by [11].

III. Measurement of Average SAR in Man Models

Hollow Styrofoam molds were used to hold liquid synthetic tissue for the determination of average SAR in man models. The mold halves, before being glued together, are illustrated in Fig. 1. The halves were joined with a liquid-tight seal, and liquid synthetic tissue was poured in. The forms consisted of 5.44-scaled models of a standing adult man (full-scale height = 171 cm) and a child (full-scale height = 86 cm), with arms down. The full-scale figure was used to reflect a worst-case situation involving exposure of a small man or a woman (SAR decreases with an increase in size at 450-MHz exposure). Each model was exposed for about 20–60 s in the anechoic chamber to 2450-MHz radiation fields of 750-mW/cm^2 incident power density at a distance of 140 cm from a standard gain horn. After exposure the average rise in temperature in the model was measured with a thermocouple; the heat loss during the several minutes needed for the measurements was negligible. The SAR for a full-scale man was obtained by multiplication of the SAR calculated for the model by the scaling factor of 5.44.

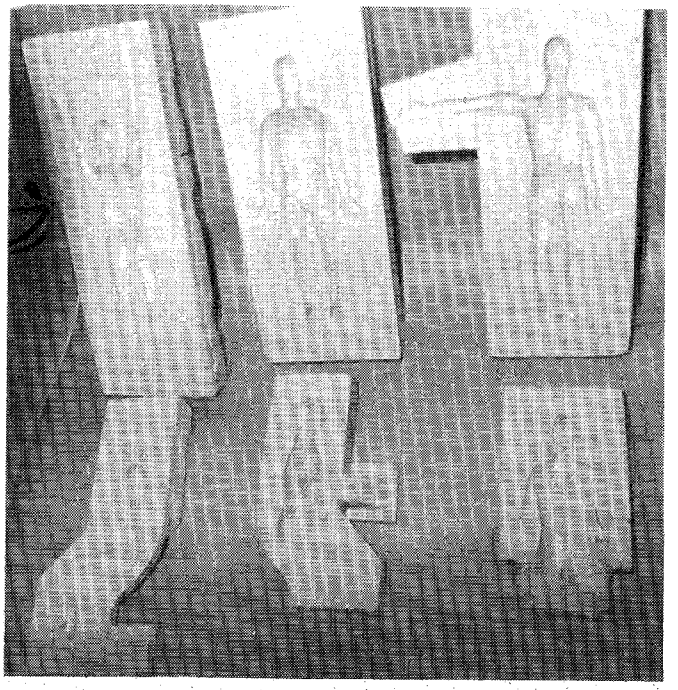

Fig. 1. Scale models of man used for average SAR and SAR distribution measurements.

TABLE II
Measured Average SAR in Scale Models of Man Under Different Exposure Orientations and Body Postures

Position	SAR (W/kg per 1 mW/cm^2) Adult (1.71 m) Muscle Model	Child (0.86 m) Muscle Model	Adult Mixed Model
Standing			
Facing source (EHK)	0.050	0.164	0.059
Back to source (-EHK)	0.053	0.175	0.057
Left Side to source (EKH)	0.041	0.187	0.046
Lying on Back			
Head to source (-KHE)	0.049	0.095	0.050
Feet to source (KHE)	0.050	0.095	0.048
Left Side to source (HKE)	0.041	0.061	0.042
Lying on Left Side			
Facing source (HEK)	0.049	0.109	0.054
Head to source (-KEH)	0.053	0.158	0.054
Feet to source (KEH)	0.063	0.165	0.061

*Scaling Factor—5.44; operating frequency—2450 MHz; simulated frequency—450 MHz.

SAR distributions were measured for 12 primary orientations of the model man with respect to the incident field. These primary polarizations were designated, using the

TABLE III
AVERAGE SAR (W/kg) VALUES FOR 1.71-m-TALL MAN (WITH HOMOGENEOUS-MUSCLE BODY) EXPOSED TO 1-mW/cm^2, 450-MHz RFR, UNDER DIFFERENT EXPOSURE EXPOSURE POLARIZATIONS AND BODY POSTURES

Polarization	Orientation	Posture			
		ARMS DOWN	ARMS UP	R-ARM OUT	
HEK	Lying on left side--facing source	0.042	0.047	0.044	
-HEK	Lying on left side--back to source	0.040	0.046	0.045	
HKE	Lying on back--left side to source	0.049	0.046	0.052	
-HKE	Lying on back--right side to source			0.055	
KEH	Lying on left side--feet to source	0.061	0.070	0.055	
-KEH	Lying on left side--head to source	0.050	0.071	0.048	
KHE	Lying on back--feet to source	0.053	0.058	0.048	
-KHE	Lying on back--head to source	0.049	0.056	0.054	
		Standing			Sitting
EHK	Facing source	0.050	0.055	0.051	0.057
-EHK	Back to source	0.046	0.053	0.047	0.056
EKH	Left side to source	0.038	0.039	0.036	0.057
-EKH	Right side to source			0.040	0.060

nomenclature of [2], by considering a coordinate system oriented with respect to the model man, with the x axis parallel to the long axis of the body, the y axis parallel to the frontal plane, and the z axis perpendicular to the frontal plane. Then the polarization was defined by which of the field vectors $\boldsymbol{E}$, $\boldsymbol{H}$, and $\boldsymbol{k}$ were parallel to the x, y, and z axes. Thus, *EHK* polarization was the orientation in which $\boldsymbol{E}$ lies along x, $\boldsymbol{H}$ lies along y, and $\boldsymbol{k}$ lies along z. Since man is asymmetrical from front to back, the six polarizations specified for the ellipsoidal model in [2] had to be considered, plus six others. If the *EHK* and *HEK* polarizations are assumed to correspond to exposures of the man facing the source, then $-EHK$ and $-HEK$ become exposures of the man with his back to the source. Likewise, if *EKH* and *HKE* represent exposures with the left side to source, $-EKH$ and $-HKE$ will correspond to exposures with the right side to the source. Finally, *KEH* and *KHE* will correspond to exposures with the head toward the source, and $-KEH$ and $-KHE$ will correspond to exposures with the feet toward the source.

Results of the first series of measurements are listed in Table II where each datum represents the average of several measurements normalized to correspond to an exposure level of 1 mW/cm^2. The largest variation was less than 10 percent. The average SAR measured for the composite-tissue model consisting of fat and muscle (with two-thirds the conductivity of muscle) was slightly higher than or equal to that measured for the 100-percent muscle model for all positions. The measured maximum average SAR for the child for all orientations was much higher than that for the adult (e.g., 0.187 W/kg versus 0.063 W/kg), which is expected since the frequency is closer to the resonance frequency for the child.

Another series of scale-model measurements was conducted for determination of the average SAR values for man when exposed in a standing position, with arms down, or both arms raised, or one arm extended to the right, and when exposed sitting. The results are shown in Table III.

IV. COMPUTERIZED THERMOGRAPHIC SYSTEM

A computerized thermographic system was developed to facilitate analysis of the large number of thermograms required to map the SAR distributions in man exposed to RFR under many possible conditions. Thermograms were taken of scale models of man similar to those used for the measurements of average SAR, shown in Fig. 1, but consisting of gelled synthetic muscle tissue with scaled conductivity. The technique was as described by [5], and analysis was according to the method discussed in the same reference and a newly developed computer method discussed below.

A more modern interactive-computer approach to the thermographic-recording analysis was implemented for assessment of SAR distribution. The AGA thermovision 680 system was interfaced with an AGA-supplied Oscar digitizer-digital tape-recording system. The system was used to digitize and store thermographic images, as well as to provide interfacing to a computer. Images could be recorded at will or recorded automatically over a selected sampling interval. The images could then either be played back and analyzed on the thermography system with its analog data-processing features or be transferred to digital tape and then to a computer. When the digital tape-recording system was interfaced with a PDP 11/34 computer, its graphics terminal and the graphics plotter could be used for analysis of the dosimetry thermograms. Magnetic tape was transported from the thermograph laboratory to the computer room for general image processing by software specially developed for detailed computer-image analysis. The analytical system based in part on the SOFTA soft-

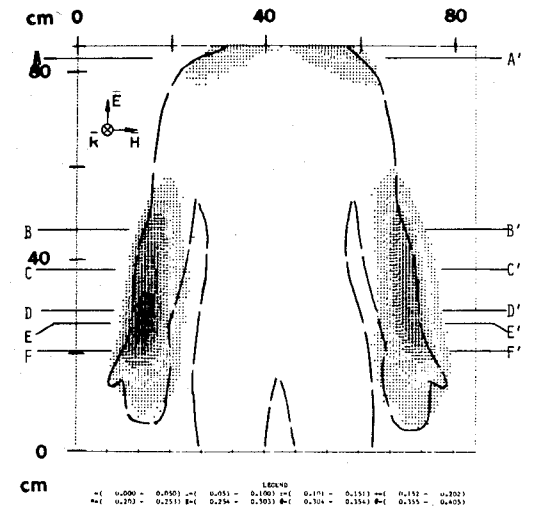

(a)

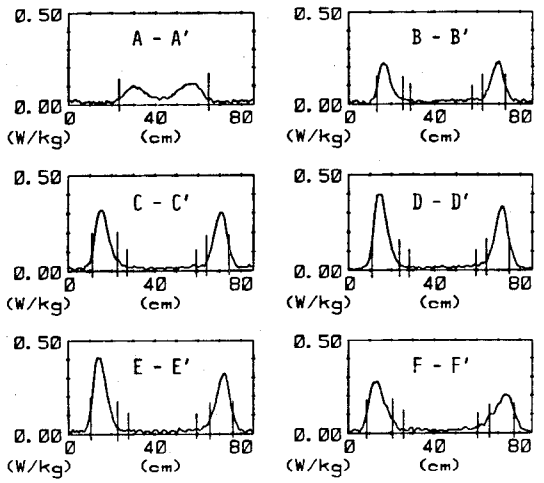

(b)

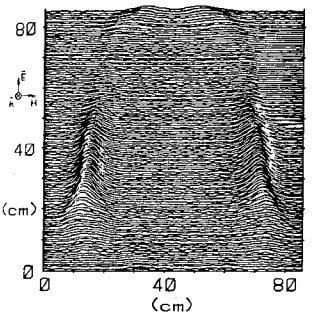

(c)

Fig. 2. (a) Computer-processed gray-scale plot of SAR's for model man exposed to *EHK*-polarization electromagnetic radiation (midbody closeup). (b) Computer-processed single-profile scans of SAR's for model man exposed to *EHK*-polarization electromagnetic radiation (midbody closeup). (c) Computer-processed multiple-profile scan of SAR's for model man exposed to *EHK*-polarization electromagnetic radiation (midbody closeup).

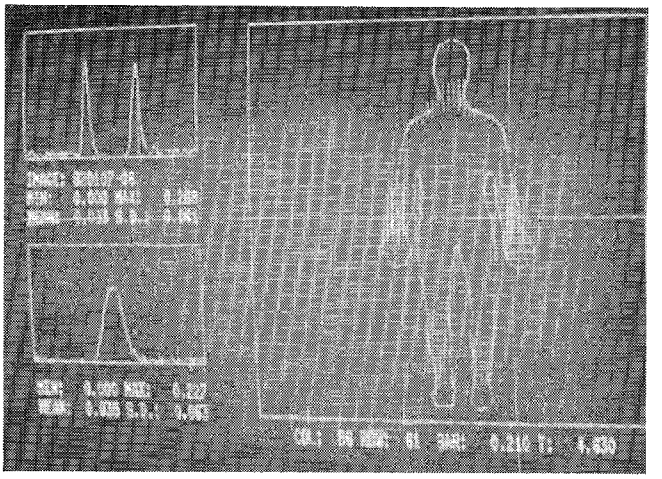

Fig. 3. Light-pen selection of point on image where horizontal and vertical SAR scans are desired.

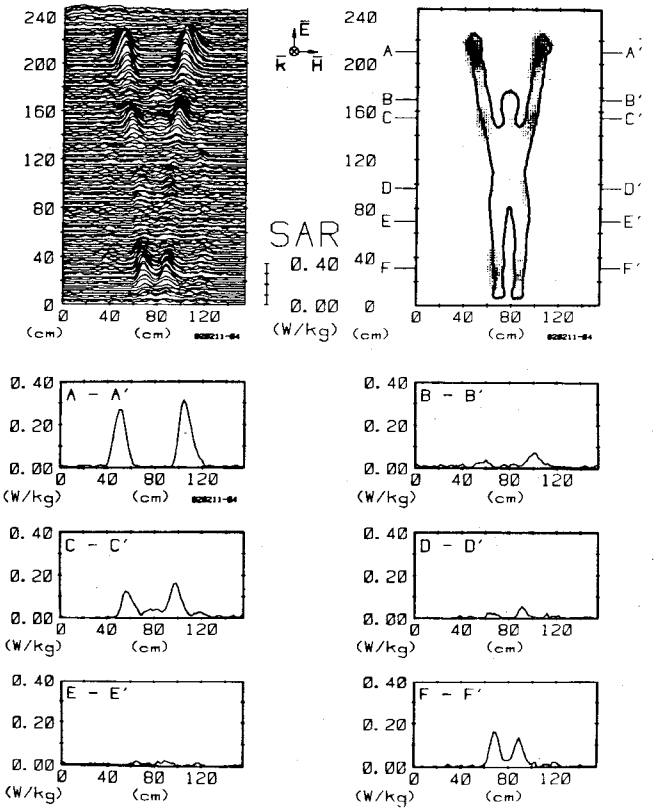

Fig. 4. Computer-processed whole-body thermograms expressing SAR patterns for man with arms up exposed to 1-mW/cm^2 450-MHz radiation with *EHK* polarization.

ware available from AGA Corporation was semi-interactive, enabling the operator to identify exactly which regions, in which images, were of interest. A 12-parameter intraregional statistical analysis could then be made of these regions and in any selected region, the following could be determined: highest and lowest SAR values, range, median, average, variance, and skewness of distribution; area of region; parameter, shape factor, geometric centroid, and percentage of total image observed. The software was arranged to enable tailoring to specific applications by selection and elimination of various subroutines. Algorithms were added to enable the computer to perform automatic interpretation and analysis. This system significantly accelerated the thermographic analysis of SAR distribution patterns and improved the reliability of data.

The graphics system employed the Hewlett/Packard 7220 flatbed plotter and the Qume Spring-5 printer. Both served as peripherals to the PDP 11/34 minicomputer. The HP-plotter output consisted of four basic types of plots: gray-scale, contour, multiple-profile, and single-profile

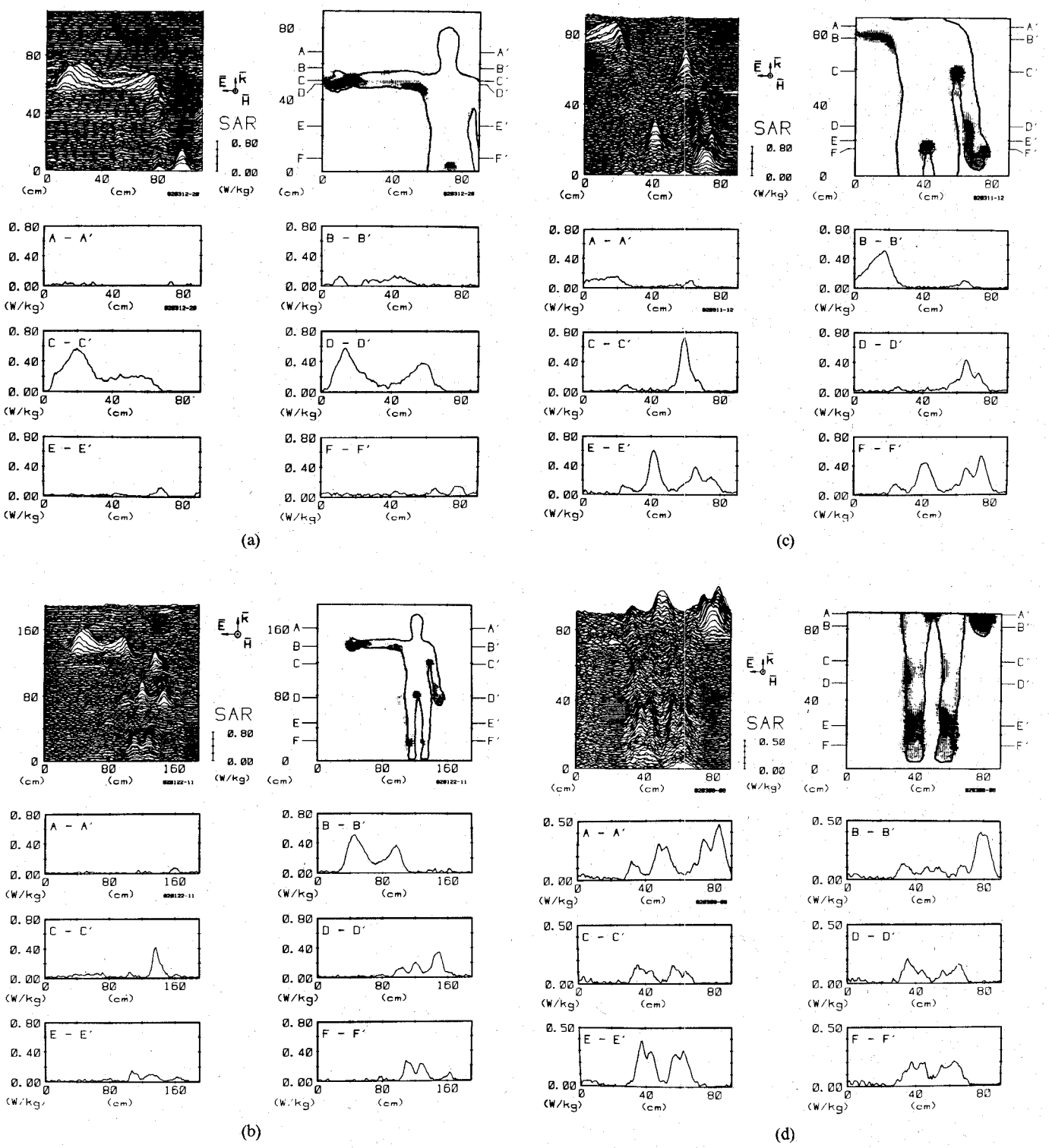

Fig. 5. (a) Computer-processed whole-body thermograms expressing SAR patterns for man with one arm extended exposed to 1-mW/cm^2 450-MHz radiation with *KEH* polarization. (b) Computer-processed upper-body thermograms expressing SAR patterns for man with one arm extended exposed to 1-mW/cm^2 450-MHz radiation with *KEH* polarization. (c) Computer-processed midbody thermograms expressing SAR patterns for man with one arm extended exposed 1-mW/cm^2 450-MHz radiation with *KEH* polarization. (d) Computer-processed lower-body thermograms expressing SAR patterns for man with one arm extended exposed to 1-mW/cm^2 450-MHz radiation with *KEH* polarization.

scans. The Qume-printer output consisted of gray-scale printouts showing the different areas of heating as varying shades of gray.

A processed gray-scale plot of the body midsection is reproduced in Fig. 2(a), and SAR is shown along specific scan lines (B-scans) in the digitized thermograph in the scans in Fig. 2(b). Each thermograph is made up of 128 scan lines. All B-scan plots are labeled to indicate the proper point of comparison with a gray-scale plot of the same image. Profile plots are composed of multiple B-scans, as shown in Fig. 2(c), presenting a sort of relief map of SAR over the thermographed object. The plot can be limited to any rectangular area of the image so the analyst can expand areas of interest for more detailed examination. Gray-scale plots are printouts that display heating in eight different shades, each shade of gray representing a specific

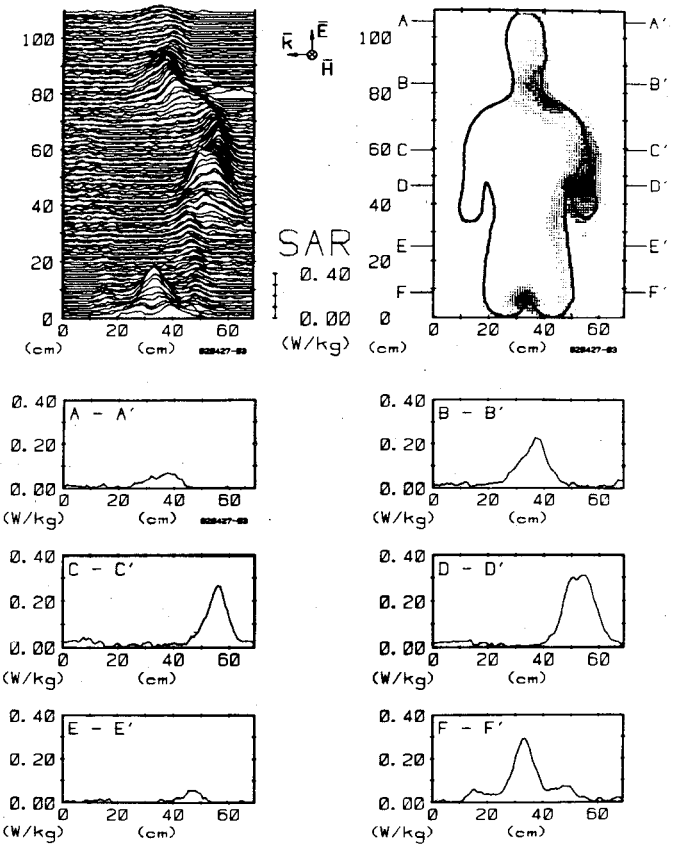

Fig. 6. Computer-processed whole-body thermograms expressing SAR patterns for man sitting (frontal plane) exposed to 1-mW/cm^2 450-MHz radiation with *EKH* polarization.

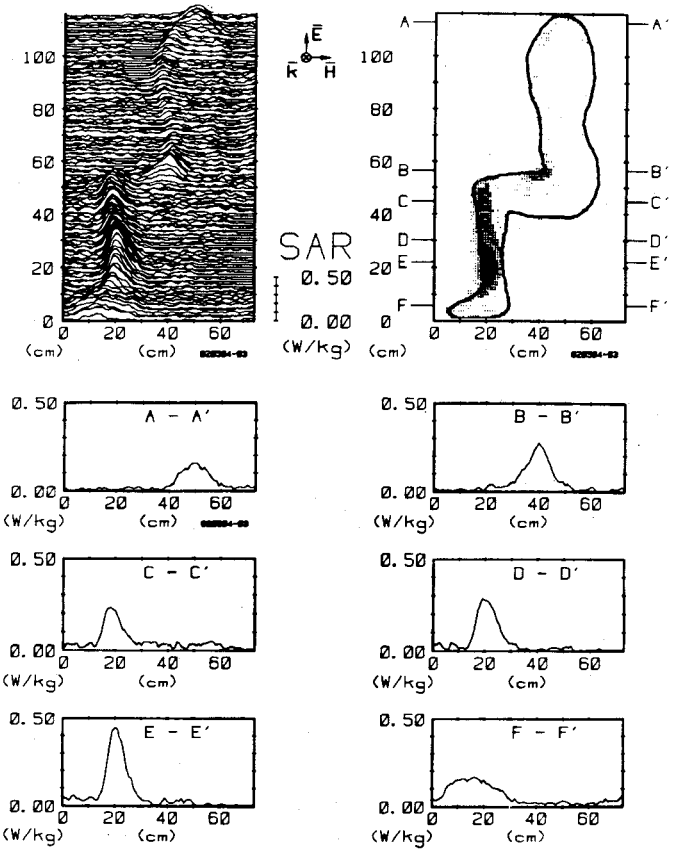

Fig. 7. Computer-processed whole-body thermograms expressing SAR patterns for man sitting (sagittal plane through leg) exposed to 1-mW/cm^2 450-MHz radiation with *EHK* polarization.

heating (SAR) range. The SAR ranges are displayed at the bottom of each plot, as shown in Fig. 2(a). For each exposure the user may also display the plot in terms of temperature, temperature change, SAR, or current density.

The data have been stored in large computer data files in the Bioelectromagnetics Research Laboratory, and the results for any given exposure situation can be quickly retrieved by the interactive computer program. Through an interactive program and the use of a light-pen, the boundary curve is fitted to the thermographic image of the highlighted unfilled model and stored in the computer for later use in the analysis. The computer fitting eliminates any error due to changes in image size or shape owing to variation with distance between the thermographic camera and the object or as a result of aberration of the camera lens.

The desired image is brought onto the screen from the file. An interactive command places the boundary around the image. Another interactive command enables the analyst to touch any point on the image with the light-pen; then the pixel column number, row number, SAR per mW/cm^2, and temperature change for the actual measurement will appear at the bottom of the screen. Another command displays on the screen a complete horizontal–vertical scan of the SAR. Through any point touched by the light-pen, the computer gives the mean, maximum, average, and

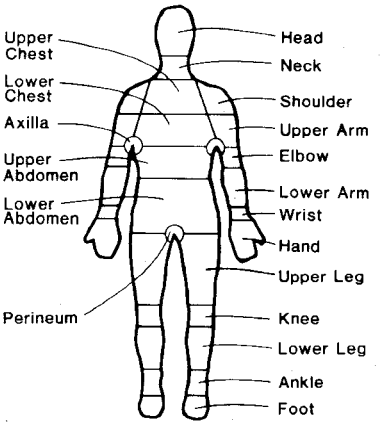

Fig. 8. Regions of body where maximum SAR values were determined from closeup thermograms. (Values are tabulated in Tables IV–VII).

standard deviation of the SAR's along the scan (Fig. 3). Information of interest can be filed or printed in hard-copy form as described previously and in the following sections.

V. SAR Distribution Patterns

Thermographs were obtained for various exposed models as described by [5], [6]. Except for being filled with the gelled synthetic tissue instead of liquid, the models were exposed in much the same way as for the calorimetric

TABLE IV
MAXIMUM SAR VALUES (W/kg) FOR MAN EXPOSED ERECT, WITH ARMS DOWN, TO 1-mW/cm^2, 450-MHz RFR, UNDER DIFFERENT EXPOSURE POLARIZATIONS

Body Part	Polarization									
	EHK	-EHK	EKH	HEK	-HEK	HKE	KEH	-KEH	HKE	-KHE
Head	.084	.100	.108	.061	.074	.150	.076	.164	.065	.249
Neck	.110	.150	.188	.032	.033	.032	.100	.164	.069	.024
Shoulder	.114	.100	.143	.066	.081	.056	.064	.279	.079	.048
Upper Chest	.099	.080	.055	.000	.000	.003	.028	.095	.049	.014
Upper Arm	.056	.056	.211	.140	.120	.048	.080	.115	.015	.010
Lower Chest	.021	.002	.128	.009	.000	.020	.032	.012	.060	.011
Axilla	.032	.020	.120	.154	.167	.057	.715	.111	.016	.020
Elbow	.266	.300	.300	.184	.119	.106	.214	.076	.013	.030
Upper Abdomen	.018	.006	.023	.000	.000	.816	.050	.006	.010	.016
Lower Arm	.403	.300	.270	.143	.101	.120	.484	.088	.045	.026
Wrist	.406	.250	.589	.109	.143	.10	.420	.140	.062	.029
Lower Abdomen	.020	.021	.014	.003	.000	.055	.171	.150	.000	.020
Perineum	.016	.027	.022	.219	.189	.084	.270	.030	.060	.169
Hand	.129	.084	.581	.258	.295	.135	.767	.724	.037	.244
Upper Leg	.081	.178	.207	.047	.114	.080	.150	.015	.052	.052
Knee	.187	.090	.144	.059	.076	.097	.157	.087	.049	.045
Lower Leg	.222	.108	.238	.061	.098	.050	.201	.195	.189	.053
Ankle	.230	.214	.264	.070	.101	.140	.275	.262	.090	.068
Foot	.077	.084	.113	.116	.158	.144	.138	.082	.295	.100

TABLE V
MAXIMUM SAR VALUES (W/kg) FOR MAN EXPOSED ERECT, WITH ARMS RAISED, TO 1-mW/cm^2, 450-MHz RFR, UNDER DIFFERENT EXPOSURE POLARIZATIONS

Body Part	Polarization									
	EHK	-EHK	EKH	HEK	HEK	HKE	KEH	-KEH	KHE	-KHE
Head	.076	.081	.006	.060	.095	.213	.173	.173	.085	.180
Neck	.054	.069	.045	.063	.032	.042	.031	.292	.024	.014
Shoulder	.090	.060	.178	.108	.072	.064	.501	.854	.035	.037
Upper Arm	.017	.008	.021	.032	.007	.007	.036	.005	.000	.016
Lower Chest	.077	.051	.000	.075	.063	.005	.022	.000	.000	.032
Axilla	.240	.201	.332	.048	.079	.068	.264	.101	.024	.055
Elbow	.062	.093	.153	.076	.057	.060	.351	.300	.063	.071
Upper Abdomen	.020	.051	.220	.078	.060	.097	.161	.005	.026	.029
Lower Arm	.328	.398	.550	.085	.106	.070	.169	.201	.051	.198
Wrist	.425	.437	.547	.095	.115	.061	.819	.838	.128	.216
Lower Abdomen	.065	.105	.103	.055	.038	.066	.090	.106	.031	.012
Perineum	.008	.013	.052	.326	.133	.075	1.053	.130	.003	.015
Hand	.185	.255	.463	.192	.201	.074	.674	.674	.112	.148
Upper Leg	.054	.101	.191	.060	.078	.121	.172	.130	.033	.058
Knee	.070	.191	.145	.079	.058	.135	.203	.181	.062	.060
Lower Leg	.280	.158	.227	.090	.081	.120	.238	.170	.049	.060
Ankle	.353	.295	.348	.056	.034	.090	.418	.351	.161	.152
Foot	.063	.104	.139	.104	.173	.534	.185	.149	.518	.094

average SAR measurements described before. The man models were sectioned along the central frontal planes to form front and back half-sections so the SAR patterns could be seen in the head, neck, thorax, arms, and legs. Some of the sitting models were sectioned through the sagittal plane so the SAR patterns in the torso, head, neck, arms, and legs could also be obtained.

The models were exposed to 2450-MHz radiation fields in the anechoic chamber for between 20 and 60 s, with input power ranging from 5 to 10 kW. Thermograms were taken before and after exposure and stored on digital tapes, then analyzed and plotted as described in the previous section.

A few examples of the thermographic data for the 5.44-scale man model exposed under various conditions are illustrated in Figs. 4–7. The whole-body scans were taken with a standard lens, and the closeup scans with a narrow-angle lens. All of the closeup thermographic data obtained from the images cannot be presented in this paper, but maximum SAR values at various portions of the body (Fig. 8) obtained from the closeup thermograms and are tabulated in Tables IV through VII.

VI. DISCUSSION

The average SAR's for man exposed to 450 MHz in the current project are compared in Table VIII with data obtained previously by our group and other investigators. When phantom scale models of man (dolls or figurines) are used, measured values of average SAR for all polarizations are somewhat greater than values calculated theoretically with the prolate spheroid models or computer models consisting of a finite number of blocks. For the prolate spheroid model of man, average SAR values vary from .016 to .034 W/kg, depending upon polarization. These values are consistent with the average SAR's reported for the computer block model [4]. Our measurements of the average SAR's for the 3–4-year-old child model (half the height of the man model) are also significantly (two to three times) higher than those predicted by theory with the prolate spheroid model.

The differences between the theoretical and experimental results may be further explored by comparison of the values over a broad frequency range, as shown in Fig. 9. The theoretical curve in the figure, based on the work of [10] with a human block model, is generally lower than the experimental curve derived from the work discussed in this report and our past work [6]. The data for the human block model compare much better with the experimental values for above-the-body-resonance frequencies (maximum level) than with the values for the prolate spheroid model, given in Table VIII. To gain a better understanding of these differences, additional measurements of average SAR were made for frequencies below resonance using the scale models (plotted as dots or circles in Fig. 9). These measurements required a different model-exposure technique, discussed in the Appendix.

Additional data, for very low to medium frequencies 10 kHz–3 MHz were obtained for the below-resonance curve from [9], who used current distribution measurements from metalized full-scale models of man exposed to 60 Hz [1] and current, potential, and resistance measurements from a live human subject with 60-Hz–300-kHz currents passing axially through the body. Guy and Chou's data [9], denoted on the curve by hexagons, seem to be consistent with our scale-model measurements.

As pointed out by [9], the shape of the model especially plays an important role in determining the average SAR during exposure. At frequencies significantly below body resonance, most energy absorption is in the lower legs since

TABLE VI
MAXIMUM SAR VALUES (W/kg) FOR MAN EXPOSED ERECT, WITH RIGHT ARM EXTENDED, TO 1-mW/cm^2, 450 MHz RFR, UNDER DIFFERENT EXPOSURE POLARIZATIONS

Body Part	Polarization											
	EHK	-EHK	EKH	-EKH	HEK	-HEK	HKE	-HKE	KEH	-KEH	KHE	-KHE
Head	.075	.123	.121	.051	.108	.062	.147	.188	.000	.204	.064	.304
Neck	.106	.123	.193	.030	.072	.046	.032	.028	.000	.146	.044	.038
Shoulder	.115	.109	.088	.029	.051	.056	.087	.038	.124	.565	.026	.069
Upper Chest	.000	.026	.000	.000	.018	.000	.004	.000	.000	.000	.000	.036
Upper Arm	.123	.105	.261	.246	.111	.070	.067	.073	.238	.174	.040	.093
Lower Chest	.000	.000	.000.	.130	.043	.000	.006	.057	.024	.000	.000	.012
Axilla	.061	.074	.289	.356	.118	.167	.079	.043	.661	.116	.017	.036
Elbow	.245	.248	.402	.369	.100	.079	.077	.072	.136	.275	.035	.054
Upper Abdomen	.000	.000	.000	.173	.000	.000	.052	.036	.152	.080	.000	.000
Lower Arm	.373	.321	.448	.246	.364	.217	.111	.098	.306	.433	.054	.098
Wrist	.353	.345	.605	.624	.532	.456	.107	.134	.577	.778	.061	.073
Lower Abdomen	.000	.019	.013	.024	.025	.000	.081	.073	.029	.000	.000	.012
Perineum	.009	.008	.014	.048	.224	.129	.053	.024	.411	.042	.459	.009
Hand	.230	.162	.725	.526	.294	.162	.134	.089	.512	.573	.363	.085
Upper Leg	.049	.138	.188	.173	.076	.114	.086	.069	.147	.000	.165	.029
Knee	.094	.132	.185	.159	.113	.099	.062	.078	.162	.063	.136	.039
Lower Leg	.246	.126	.275	.144	.108	.125	.072	.090	.198	.105	.212	.055
Ankle	.272	.240	.290	.254	.123	.114	.149	.126	.375	.242	.199	.139
Foot	.070	.084	.105	.045	.153	.243	.386	.441	.176	.179	.300	.066

TABLE VII
MAXIMUM SAR VALUES (W/kg) FOR MAN EXPOSED, SITTING, TO 1-mW/cm^2, 450-MHz RFR, UNDER DIFFERENT EXPOSURE POLARIZATIONS

Body Part	Polarization		
	EHK	-EHK	EKH
Head	.198	.147	.138
Neck	.290	.227	.355
Shoulder	.253	.389	.469
Upper Chest	.087	.155	.072
Upper Arm	.219	.643	.476
Lower Chest	.096	.187	.077
Axilla	.245	.643	.694
Elbow	.657	.375	.635
Upper Abdomen	.116	.223	.216
Lower Arm	.242	.136	.258
Wrist	.121	.138	.290
Lower Abdomen	.076	.187	.080
Perineum	.198	.148	.466
Hand	.226	.142	.244
Upper Leg	.159	.121	.113
Knee	.154	.244	.222
Lower Leg	.545	.396	.545
Ankle	.353	.374	.249
Foot	.234	.161	.087

the shape and size of the legs play an important part in the absorption mechanism.

A.) Average SAR

In [2], the variation of average SAR with polarization appears to be minimum at the frequency of 450 MHz. This phenomenon has been confirmed experimentally in this study. Based on 41 values of measured average SAR, presented in Tables II and III, for a homogeneous-muscle man model exposed under different posture and polarization conditions, the statistics for the SAR (W/kg) for an exposure level of 1 mW/cm^2 are as follows:

No. of values	Mean	Standard deviation	Minimum value	Maximum value
41	0.0498	0.0075	0.0365	0.0714

From these data, it can be assumed that, regardless of the exposure conditions for man—whether the polarization is vertical, horizontal, or circular; or the posture is standing, supine, or sitting; or the arms are extended or not—the average SAR remains relatively constant at a level of approximately 0.05 W/kg for a 1-mW/cm^2 exposure level. This SAR level is a factor of eight below the level used as a basis for the ANSI C95.1-1982 RFR standard.

B.) Maximum SAR and SAR Distribution

Figs. 4–7 and Tables IV–VII indicate that, in the body of a man exposed at 450 MHz, the SAR is far from uniform and reaches values as high as 13 times the average.

In general, when the man is exposed with the electric-field vector parallel to the body, SAR is maximal in the narrow cross sections, such as the neck, wrists, and ankles, with the highest levels in the wrists. For frontal or back exposures under these conditions, the SAR patterns are symmetrical with respect to the sagittal plane, and typical maximal

TABLE VIII
COMPILATION OF THEORETICAL AND EXPERIMENTAL DATA ON AVERAGE SAR FOR HUMAN EXPOSURE TO FREQUENCIES NEAR OR EQUAL TO 450-MHz AT 1-mW/cm^2

Investigator, frequency, and model	ϵ'	σ(S/m)	SAR (W/kg) Exposure Polarization EKH	EHK	HEK	HKE	KEH	KHE	-KEH	-KHE
Durney et al. (1978)										
450-MHz										
Theoretical:										
Prolate spheroid										
Avg man	36	0.82	.034	.034	.030	.030	.016	.016	.016	.016
Skinny man	36	0.82	.049	.049	.036	.036	.022	.022	.022	.022
5-yr-old child	36	0.82	.062	.062	.042	.042	.031	.031	.031	.031
1-yr-old child	36	0.82	.094	.094	.043	.043	.052	.052	.052	.052
Infant	36	0.82	.125	.125						
Gandhi (1977)										
462.3-MHz										
Measured:	Unknown	Unknown								
Human figurine	saline	saline	.045		.044		.063			
Gandhi (1979)										
462.3-MHz										
Theoretical:										
Computer avg man	36	0.82		.035						
Measured:	Unknown	Unknown								
Human figurine	saline	saline							.056	.057
Guy et al. (1978)										
442-MHz										
Measured:										
Human doll	58.9	1.68	.041	.046	.049	.049	.069	.043	.057	.039
(Current project)										
Human doll	50.2	1.18	.041	.050	.049	.041	.063	.050	.053	.049
Adult	33.1	0.89	.046	.059	.054	.042	.061	.048	.054	.050
450-MHz										
Measured:										
3-4-yr-old child	50.2	1.18	.187	.164	.108	.061	.165	.094	.158	.095

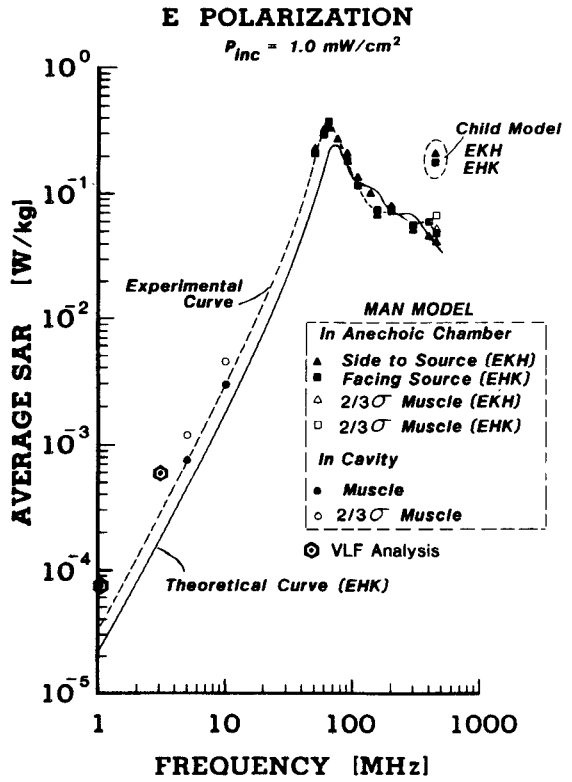

Fig. 9. Comparison of theoretical and experimentally measured whole-body average SAR's for realistic man models exposed at various frequencies.

SAR values are 0.1, 0.4, and 0.3 W/kg for the neck, wrists, and ankles, respectively. When the exposures are from the side, the patterns become asymmetrical with respect to the sagittal plane. Maximal values for SAR are on the exposed side, with levels reaching 0.2, 0.6, and 0.3 W/kg in the neck, wrists, and ankles, respectively.

When the man is exposed with the electric field perpendicular to the long axis of the body but parallel to the broad side, localized SAR can occur in the perineal and axillar areas of the body owing to sharp diversion of the RF currents around the wedge-shaped discontinuities of the body. In general, when the electric field is not tangent to the apex of such discontinuities, this localized SAR will not occur. The data on SAR distribution show that, even though the average SAR does not significantly vary with position or posture, the pattern of the localized SAR will change radically. Most of the maximal SAR levels, however, occur in the limbs and in the perineal and axillar areas, depending on exposure conditions.

APPENDIX A

MEASUREMENT OF AVERAGE SAR VALUES BELOW BODY-RESONANCE FREQUENCIES

A special exposure system is needed for making average SAR measurements in models to simulate human exposure to frequencies below the body-resonance frequency. We

used a 57.3-MHz resonant-cavity system to expose scale models of man to simulate exposures of man to high-frequency (HF) electric fields, the greatest contributor to SAR at frequencies below body resonance. Though similar work had been reported previously [6], the new cavity was much improved and provided greater accuracy and more flexibility in the choice of model sizes and shapes [8]. Also, in the latest measurements we compared homogeneous muscle tissues and tissues with two-thirds conductivity of muscle [2]. By adjusting the model conductivity in the appropriate manner, we exposed models to 57.3-MHz electric fields in the cavity to simulate the exposure of a full-scale man to 5–10 MHz. For example, the conductivity for the 10-MHz exposure for the two-thirds muscle mixture is given by

$$\sigma = (57.3\ \text{MHz}/10\ \text{MHz}) \times 2/3 \times 0.625 = 2.38\ \text{S/m}.$$

After exposing the models, we measured the temperature change in each model and calculated the SAR. From the SAR, denoted by W (57.3 MHz), measured at the 57.3-MHz exposure frequency, we can calculate the SAR for exposure at the full-scale frequency, W (10 MHz), by the following equation:

$$W\ (10\ \text{MHz}) = W\ (57.3\ \text{MHz})/5.73.$$

Theoretically the SAR, W (f MHz), at any other HF-band frequency (f MHz, significantly below the body resonance frequency) may be calculated in terms of the 10-MHz exposure by the following equation:

$$W\ (f\ \text{MHz}) = W\ (10\ \text{MHz}) \times [\sigma(10\ \text{MHz})/\sigma(f\ \text{MHz})] \times (10\ \text{MHz}/f\ \text{MHz})^2$$

where σ (10 MHz) is the conductivity of the actual tissue of the full-scale man at 10 MHz, and $\sigma(f$ MHz) is the conductivity at any other frequency in the HF band.

The SAR's as measured for 5–10 MHz and the values as extrapolated to other frequencies are shown in text Fig. 9, represented by the dot and circle symbols, respectively.

References

[1] D. W. Deno, "Current induced in human body by high-voltage transmission line electric field—Measurement and calculation of distribution and dose," *IEEE Trans. Power App. Syst.*, vol. PAS-96, no. 5, pp. 1517–1527, 1977.

[2] C. H. Durney, C. C. Johnson, P. W. Barber, H. Massoudi, M. F. Iskander, J. L. Lords, D. K. Ryser, S. J. Allen, and J. C. Mitchell, *Radiofrequency Radiation Dosimetry Handbook*, 2nd ed. SAM-TR-78-22, May 1978.

[3] O. P. Gandhi, E. L. Hunt, and J. A. D'Andrea, "Deposition of electromagnetic energy in animals and in models of man with and without grounding and reflector effects," *Radio Sci.*, vol. 12, no. 6S, pp. 39–47, 1977.

[4] O. P. Gandhi, M. J. Hagmann, and J. A. D'Andrea, "Part-body and multibody effects on absorption of radio-frequency electromagnetic energy by animals and by models of man," *Radio Sci.*, vol. 14, no. 6S, pp. 23–30, 1979.

[5] A. W. Guy, M. D. Webb, and C. C. Sorensen, "Determination of power absorption in man exposed to high frequency electromagnetic fields by thermographic measurements on scale models," *IEEE Trans. Biomed. Eng.* vol. BME-23, no. 5, pp. 361–371, 1976.

[6] A. W. Guy, M. D. Webb, A. F. Emery, and C. K. Chou, "Measurement of power distribution at resonant and nonresonant frequencies in experimental animals and models," Scientific Rep. 11, Bioelectromagnetics Res. Lab., U. Washington, Seattle, WA. USAFSAM Contract F41609-76-C-0032 Final Rep., Brooks AFB, TX.

[7] A. W. Guy, C. K. Chou, R. B. Johnson, and L. L. Kung, "Study of effects of long-term low-level RF exposure on rats: A plan," *Proc. IEEE*, vol. 68, no 1, pp. 92–97, 1980.

[8] A. W. Guy, S. Davidow, G. Y. Yang, and C. K. Chou, "Determination of electric current distributions in animals and humans exposed to a uniform 60-Hz high intensity electric field," *Bioelectromagn.* vol. 3, no. 1, pp. 47–71, 1982.

[9] A. W. Guy and C. K. Chou, "Hazard analysis: Very low frequency through medium frequency range," Bioelectromagnetics Res. Lab., Dept. Rehabilitation Medicine, U. Washington, Seattle, WA, USAFSAM Contract F33615-78-D-0617, Task 0065, Final Rep., 1982.

[10] M. J. Hagmann, O. P. Gandhi, and C. H. Durney, "Numerical calculation of electromagnetic energy deposition for a realistic model of man," *IEEE Trans. Microwave Theory Tech.*, vol. MTT-27, no. 9, pp. 804–809, 1979.

[11] H. S. Ho and A. W. Guy, "Development of dosimetry for RF and microwave radiation. II: Calculations of absorbed dose distributions in two sizes of muscle-equivalent spheres," *Health Phys.*, vol. 29, pp. 317–324, 1975.

[12] J. A. Stratton, *Electromagnetic Theory*. New York and London: McGraw-Hill, 1941, pp. 488–489.

Arthur W. Guy (S'54–M'57–SM'74–F'77) was born in Helena, MT, on December 10, 1928. He received the B.S. degree in 1955, the M.S. degree in 1957, and the Ph.D. degree in 1966, all in electrical engineering from the University of Washington, Seattle.

From 1947 to 1950 and from 1951 and 1952, he served in the U.S. Air Force as an Electronic's Technician. Between 1957 and 1964 he was a Research Engineer in the Antenna Research Group, Boeing Aerospace Co., Seattle, WA. While there, his field included research on broad-band and microwave devices, surface wave antennas, propagation through anisotropic dielectrics, and antennas buried in lossy media. Between 1964 and 1966 he was employed by the Department of Electrical Engineering, University of Washington, conducting research on VLF antennas buried in polar ice caps. At that

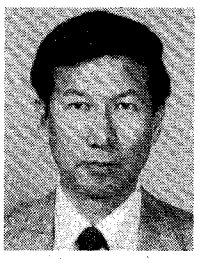

Chung-Kwang Chou (S'72–M'75) was born in Chung-King, China, on May 11, 1947. He received the B.S. degree from the National Taiwan University in 1968, the M.S. degree from Washington University, St. Louis, MO, in 1971, and the Ph.D. degree from the University of Washington, Seattle, in 1975, all in electrical engineering.

During his graduate study at the University of Washington, he had extensive training in both electromagnetics and physiology. He spent a year as an NIH Post-Doctoral Fellow in the Regional Primate Research Center and the Department of Physiology and Biophysics at the University of Washington, and became an Assistant Professor in the University's Department of Rehabilitation Medicine, in 1977. Currently, he is a Research Associate Professor in the Center for Bioengineering and Department of Rehabilitation Medicine, as well as Associate Director of the Bioelectromagnetics Research Laboratory. He is engaged in teaching and research in electromagnetic dosimetry, exposure systems, biological effects of microwave exposure, and RF hyperthermia for cancer treatment. He is a consultant for the NCRP's Scientific Committee 53 on the biological effects and exposure criteria for radio frequency electromagnetic fields, and he has also served on the ANSI Subcommittee C95.4 since 1978, and is now the chairman of 3-kHz–3-MHz working group.

Dr. Chou was the Chapter Chairman of IEEE's Seattle Section on Antennas and Propagation/Microwave Theory and Technique in 1981–1982. He is now on the Board of Directors of the Bioelectromagnetics Society. In 1981, he received the first special award for the decade of the 70's for contributions in medical and biological research from the International Microwave Power Institute. He is a member of BEMS, AAAS, IMPI, the Radiation Research Society, Tau Beta Pi, and Sigma Xi.

time, he also served as Consultant to the Department of Rehabilitation Medicine, working on problems associated with the effect of electromagnetic fields on living tissue. In 1966, he joined the faculty of the Department of Rehabilitation Medicine. Presently, he is a Professor in the Center for Bioengineering, has a joint appointment as Professor in Rehabilitation Medicine and adjunct Professor in Electrical Engineering. He is involved in teaching and research in the area of biological effects and medical applications of electromagnetic energy.

Dr. Guy is a member of COMAR, ANSI C-95 Committee, and Chairman of the 1970–1982 Subcommittee IV that developed the protection guides for human exposures to radiofrequency fields in 1974 and 1982, NCRP, and chairman of Scientific Committee 53 responsible for biological effects and exposure criteria for radiofrequency fields, Armed Forces National Research Council Committee on Vision Working Group 35, Commission A Radio Measurement Methods and URSI, ERMAC, and the EPA Scientific Advisory Board Subcommittee on Biological Effects of Radiofrequency Fields. He also serves as a consultant to the NIEHS on the USSR–U.S. Environmental Health Cooperative Program and was a member of the NIH Diagnostic Radiology Study Section 1979–1983. He is a member of the editorial boards of the *Journal of Microwave Power* and IEEE TRANSACTIONS ON MICROWAVE THEORY AND TECHNIQUES.

Dr. Guy holds memberships in Phi Beta Kappa, Tau Beta Pi, and Sigma XI. He is also a member of the American Association for the Advancement of Science, and is current President of the Bioelectromagnetics Society.

Barry Neuhaus was born on August 13, 1947, in Alton, IL. He received the B.S. degree in mathematics from the University of Washington, Seattle, in 1973.

In 1975, he became involved with the development of an interactive real-time radar track analysis program for the AWACS program at Boeing, and in 1978, joined COMTEK Research to work on an interactive shipboard electronics countermeasure program for the Navy. From 1980 to 1983, he was employed by the Bioelectromagnetics Research Laboratory at the University of Washington, and while there, he worked on an automated image processing system using the PDP 11/34 to study SAR distribution in objects exposed to electromagnetic waves. Currently, he is with the National Oceanic and Atmospheric Administration, participating in the development of a computer model of the particle distribution processes in the Puget Sound water waste. His interests are computer modeling and image processing.

Human Body Impedance for Electromagnetic Hazard Analysis in the VLF to MF Band

HIROSHI KANAI, MEMBER, IEEE, INDIRA CHATTERJEE, MEMBER, IEEE, AND OM P. GANDHI, FELLOW, IEEE

Abstract—**A knowledge of the average electrical impedance of the human body is essential for the analysis of electromagnetic hazards in the VLF to MF band. The purpose of our measurements was to determine the average body impedance of several human subjects as a function of frequency. Measurements were carried out with the subjects standing barefoot on a ground plane and touching various metal electrodes with the hand or index finger. The measured impedance includes the electrode polarization and skin impedances, spread impedance near the electrode, body impedance, stray capacitance between the body surface and ground, and inductance due to the body and grounding strap. These components are separated and simplified equivalent circuits are presented for body impedance of humans exposed to free-space electromagnetic waves as well as in contact with large ungrounded metallic objects therein.**

Manuscript received October 12, 1983; revised March 4, 1984. This work was supported by the USAF School of Aerospace Medicine, Brooks Air Force Base, TX, under Contract F33615-83-R-0613.

H. Kanai is with the Department of Electrical Engineering, University of Utah, Salt Lake City, UT 84112, on sabbatical from Sophia University, Japan.

I. Chatterjee and O. P. Gandhi are with the Department of Electrical Engineering, University of Utah, Salt Lake City, UT 84112.

I. INTRODUCTION

THE HAZARD to humans due to exposure to electromagnetic (EM) waves in the VLF to MF band (10 kHz–3 MHz) is of two kinds. The first is the energy absorption as a result of direct exposure to free-space EM fields. The second is the hazard due to current flow when a human makes contact with large ungrounded metallic objects, like cars, trucks, etc., which are exposed to EM fields. This latter effect is on account of an open-circuit RF voltage induced on these insulated objects which may result in high current densities passing through a human subject upon contact. A knowledge of the average electrical impedance of the human body is essential for the evaluation of currents flowing through the body. It is also necessary to know the electrode polarization and skin impedances, and the spreading impedance near the electrode as a function of frequency for the calculation of currents.

0018-9480/84/0800-0763$01.00 ©1984 IEEE